

Transition from Rolling to Jamming in Thin Granular Layers

C. Marone,^{1,*} B. M. Carpenter,¹ and P. Schiffer²

¹*Department of Geosciences and Energy Institute Center for Geomechanics, Geofluids, and Geohazards, The Pennsylvania State University, University Park, Pennsylvania 16802, USA*

²*Department of Physics and Materials Research Institute, The Pennsylvania State University, University Park, Pennsylvania 16802, USA*

(Received 14 May 2008; published 10 December 2008)

We study the granular jamming transition for sheared layers of spherical beads ranging in thickness from 1 to 3 times the grain diameter d . As the layer thickness increases slightly above d , the measured friction jumps discontinuously from 0.02 to >0.1 , marking the transition from rolling to jamming. Above a critical layer thickness for jamming, the effective granular pressure displays a power law increase with thickness. For thin layers, friction and P increases as the packing fraction decreases near the jamming transition, in contrast to expectations for bulk granular matter.

DOI: 10.1103/PhysRevLett.101.248001

PACS numbers: 45.70.-n, 45.50.-j

Granular materials play a key role in a broad spectrum of problems ranging from industrial handling to shear in earthquake fault zones. Shear of bulk granular materials has received considerable attention, with particular focus on factors that dictate phase transitions, spatiotemporal heterogeneity of dynamical length scales, force distribution, and the jamming transition [1–11]. In the hard sphere limit, subtle changes in granular packing fraction ϕ can lead to dramatic changes in physical properties [12–17]. Several studies have investigated the critical packing fraction ϕ_c for jamming in a granular volume [14,18,19]. Fewer works have considered jamming and associated processes in thin granular layers, where boundary separation is less than a few times the average particle dimension, $\langle d \rangle$ [6,12,20]. Previous studies show reduced friction for monolayers compared to thicker layers [6] and the importance of buckling and solid-solid phase transitions for confined thin layers [12,20]. The factors that cause jamming in thin layers and the relationship between key physical properties are, however, poorly understood.

Here, we report laboratory studies of the frictional properties of thin layers of spherical grains with focus on the behavior as layer thickness h increases above $\langle d \rangle$, a monolayer. We impose constant shear velocity and infer jamming from frictional strength. Our data show that friction exhibits an abrupt transition, from rolling to jamming, over a narrow range of layer thickness and packing fraction, and we find an unusual packing fraction dependence to the measured properties as a result of the reduced dimensionality.

We studied grain layers in a double direct shear configuration (Fig. 1). Two identical granular layers were sandwiched between three mirror-smooth, hardened steel forcing blocks and sheared simultaneously with frictional contact area of 0.01 m² (all quantities reported here refer to a single layer, see Ref. [21] and references therein for details). We used type S soda-lime glass beads (Jaygo,

Inc.) and sieved them to ensure $0.050 < d$ (cm) < 0.060 . Five different configurations (Fig. 1) were investigated by constructing layers with bead mass m equal to 1.0, 1.25, 1.5, 2.0, and 3.0 times the mass of a monolayer. The monolayer mass was determined by covering the 10×10 cm² frictional surface in multiple trials, with the result $\langle m_{\text{monolayer}} \rangle = 5.14$ grams. Layers were constructed by spooning beads onto the surface of the side forcing blocks positioned horizontally in a leveling jig, while layer edges were confined by a cellophane tape fence [21]. Grains were distributed evenly over the surface but were not arranged or packed in any special way. Using the bead density (2.5 g/cm³) and assuming $\langle d \rangle = 550$ μ m, our monolayers had a solid volume of 2.056 cc and a solid fraction ϕ of

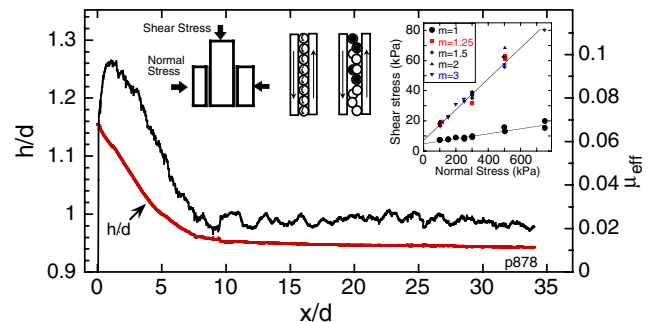


FIG. 1 (color online). (left inset) Double direct shear arrangement. Friction contact area is constant during shear. Side blocks move normal to the shear direction to maintain constant normal stress. (center inset) Sketches for two of the five layer configurations investigated. (main plot) Typical run with $m = 1$, showing the nondimensional layer thickness and friction coefficient versus nondimensional shear offset. Initial layer thickness is $1.16d$. The layer thins until it becomes a monolayer at x/d of ~ 10 . Friction reaches a peak value of 0.09 and decreases as the layer thins. Normal stress was 500 kPa for this experiment. (right inset) Kinetic frictional strength increases linearly with normal stress and is notably different for $m = 1$ and $m > 1$.

0.374. If we consider the equivalent 2D area of the beads, the 2D packing fraction of our monolayers was 0.561. Visual inspection showed that layers include ordered and disordered regions with gaps, but that “rattlers” are not present.

For each experiment, a constant normal stress was applied and maintained by servohydraulic control. Normal stress ranged from 100 kPa to 750 kPa, which is well below the crushing strength of beads (>15 MPa in this configuration). Layers were sheared in a vertical orientation (Fig. 1) with a shear displacement rate of 10 microns/s ($0.0182d/s$). Load cells were calibrated for forces as low as 10 N (100 Pa) and the *in situ* measurement resolution was 5 N. All measurements have been corrected for the gravitational force associated with the mass of the center forcing block (17.9 N) and for stretching of a latex sheet used to support the bottom of the layer (19.4 N). We report values of the effective coefficient of friction ($\mu_{\text{eff}} = \text{shear stress}/\text{normal stress}$) after correcting for an apparent cohesion of 5 kPa (Fig. 1 inset). Measured values of cohesion are consistent with small, nonzero shear strength due to elastic particle deformation for normal stresses >100 kPa. Layer thickness was measured *in situ* before shear (to $\pm 50 \mu\text{m}$) and changes in thickness during shear, which represent layer compaction or dilation, were recorded to $\pm 0.1 \mu\text{m}$. We normalize layer thickness and shear displacement, x , by $\langle d \rangle = 550 \mu\text{m}$.

Figure 1 shows representative data for shear of a monolayer, by which we mean a layer constructed with mass $m = 1$. When shear began, the layer thickness was $1.16d$ and thinning occurred over a shear displacement of $\sim 10d$ (Fig. 1). We interpret the initial thickness, $h > d$, as a result of slight particle rearrangement during transfer of the layers from the bench to the testing apparatus. Upon initiation of loading, shear stress increased rapidly and μ_{eff} exhibited a peak value before decreasing to a steady-state value of 0.02 ± 0.005 when the sample had thinned to a constant value of $h \approx d$ (Fig. 1).

As shown in Fig. 2(a), for layers thicker than a monolayer (i.e., $m > 1$), the evolution of friction with shear changed significantly. For these thicker layers, steady-state friction was reached gradually rather than exhibiting a pronounced peak strength and subsequent weakening, although the measured layer thickness versus shear was similar to that shown in Fig. 1 for a monolayer. For all experiments, steady-state kinetic friction was attained by displacements of $\sim 15d$. We define h_{ss} as the layer thickness at which μ_{eff} reached steady state.

Figure 2(b) shows the steady-state friction as a function of layer thickness, revealing a clear transition between $m = 1$ and $m = 1.25$, with μ_{eff} jumping from 0.02 to somewhat greater than 0.1. We interpret this jump as a transition from rolling to jamming. We may refine the estimate of the jamming transition (Fig. 3) by considering h_{ss} and the shear thinning characteristics of monolayers

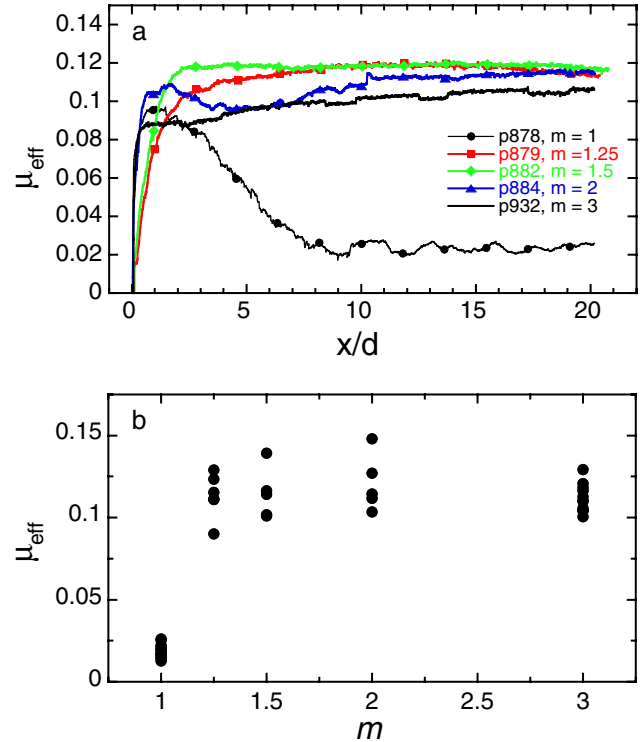


FIG. 2 (color online). (a) Representative data showing friction versus normalized shear displacement for each of the five layer configurations investigated. Only monolayers ($m = 1$) show a pronounced peak strength and subsequent weakening. Layers with mass $m \geq 1.25$ exhibit a smooth transition to steady-state kinetic friction. (b) Kinetic friction is plotted versus normalized layer mass. Friction shows a clear transition between $m = 1$ and $m = 1.25$, with values jumping from 0.02 to 0.12.

($m = 1$). The solid points in Fig. 3(a) shows steady-state friction and h_{ss} for all experiments, and the discontinuity associated with the rolling to jamming transition is again apparent. The values of $\mu_{\text{eff}} \sim 0.02$ are obtained from monolayers; the cluster of points with normalized layer thicknesses from 1.17 to 1.6 are for $1 < m \leq 2$, and the remaining points, at h_{ss}/d values above 2, are for $m = 3$ [Fig. 3(a)]. Friction values for thicker layers show some scatter but they do not vary systematically with normal stress (cf. Figure 1 inset).

The jamming to rolling transition is elucidated in Fig. 3 by the solid lines, which are raw data for shear thinning sections (e.g., Fig. 1) of two $m = 1$ experiments. These data document the form of the transition from rolling to a jammed state for $h/d > 1.17$ through both the effective friction and the packing fraction [Figs. 3(a) and 3(b)]. Figure 3(a) shows that these data cleanly connect the steady-state friction values for monolayers and thicker layers. Somewhat surprisingly, Fig. 3(b) shows that packing fraction increases as friction decreases during shear weakening, in contrast to theory and observation for bulk granular matter [13,17]. The reduction in friction with increasing packing fraction is somewhat counterintuitive,

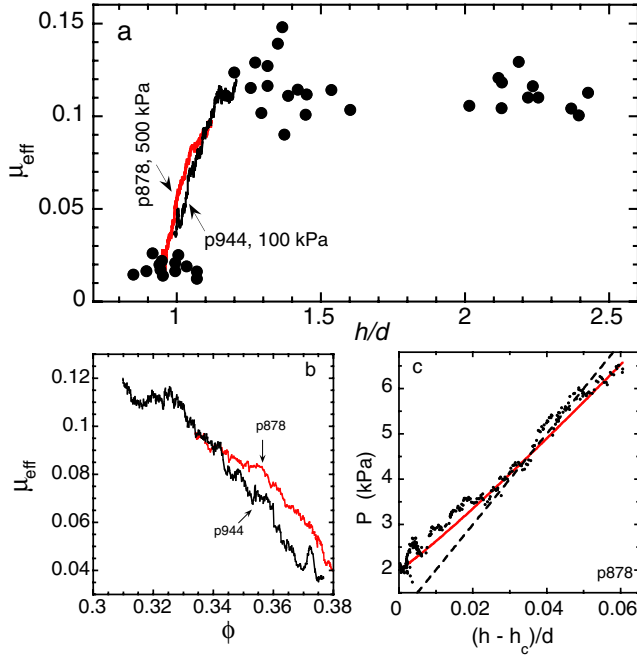


FIG. 3 (color online). Friction versus normalized layer thickness and packing fraction in the vicinity of the jamming transition. (a) Circles show friction versus h_{ss} for all experiments. Friction shows a large, discontinuous jump in the range $1.07 > h/d > 1.17$. Detailed records of friction versus layer thickness are shown for the shear thinning-weakening section (see Fig. 1) of two monolayer experiments. Data start at peak friction and extend to the point at which friction and layer thickness reach steady state. (b) Friction versus packing fraction for the data segments shown in (a). Note that friction decreases with increasing packing fraction and that the trend is quasilinear. (c) Granular pressure P versus deviation from the critical layer thickness. Solid line shows power law $[(h - h_c)/d]^\alpha$ with exponent $\alpha = 1.1$. Dashed line shows a linear law for comparison.

but consistent with a change from long-range particle interaction and jamming (possibly originating from a few grains, held up above the layer, which frustrate rolling) to rolling in a true monolayer. We note that a similar result is found in a numerical model of dense flows, where boundary shear exhibits weakening with increasing packing fraction [22].

We can also consider the granular pressure, P , which is expected to increase as a power law in the vicinity of the jamming transition [7,13,14,17]. Although we do not measure P for individual particles, we can obtain an average value by assuming that the average shear strength of the layer is proportional to P . Grains begin to roll freely when the thickness reaches h_{ss} for $m = 1$; thus, we take the critical thickness for the jamming transition to be $h_c = h_{ss}$. Figure 3(c) shows that P increases as a power law $[(h - h_c)/d]^\alpha$ with $\alpha = 1.1 \pm 0.05$ for thickness above a critical value. We cannot rule out other functional forms for $P(h)$, such as piecewise linear. A power law does better than linear, however, and the exponent we obtain is con-

sistent with theory [14], 2D experiment [17], and the expected range for Hookean ($\alpha = 1$) to Hertzian ($\alpha = 1.5$) contacts.

These same data allow us to examine the granular pressure through the jamming transition as a function of packing fraction. Theoretical studies of jamming in two and three dimensions [14] show that contact number and pressure grow as a power law of the excess 3D packing fraction $(\phi - \phi_c)$. For shear of bulk materials or thick layers, larger values of packing fraction correspond to thinner layers, so these theories would predict increasing P as layers thin below a critical value, contrary to the data of Fig. 3. This again highlights a key distinction between thin layers, where finite size effects and confined geometry are important, and the behavior of bulk granular matter. The jamming transition for bulk grains is observed as the assemblage densifies and packing fraction increases, while we observed jamming in association with a decrease in packing fraction as rolling is frustrated by layer thickening.

By further considering the packing fraction, we find that it affects the frictional strength of the layers in a nontrivial fashion. When taken together (Fig. 4), our data show that the transition from rolling to a jammed state in thin layers is not a simple function of packing fraction, which we derive from h_{ss} . For $m = 1.25$ and 1.5 layers, ϕ is in the same range as for monolayers ($0.35 < \phi < 0.41$). This is perhaps not surprising, because if $m = 1.5$ layers were packed into a monolayer ϕ would be 0.56 , which is denser than cubic packing of a layer and thus unlikely to be

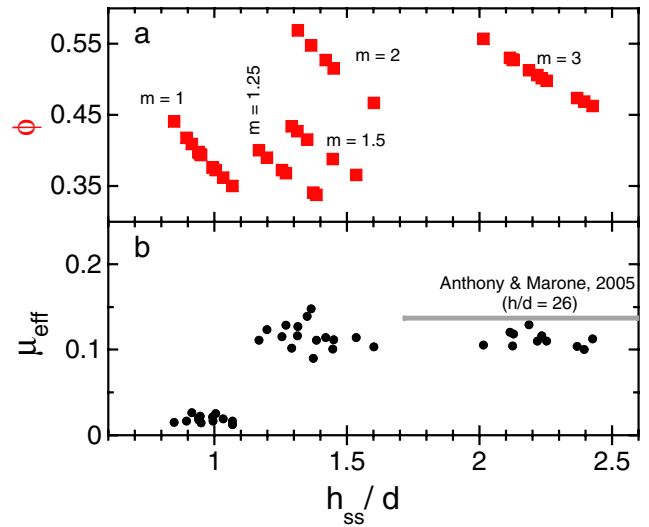


FIG. 4 (color online). Steady-state packing fraction (panel a) and friction (panel b) are plotted versus steady-state layer thickness, h_{ss} . (a) Annotations show layer mass for each experiment set. (b) Horizontal line shows steady-state friction value for thick layers of monodispersed glass beads. Note that kinetic friction for our $m \geq 1.25$ layers is nearly the same as much thicker layers. Packing fraction for layers with $m < 2$ show significant overlap.

obtained by chance. Our layers with $m = 1.5$ have an average initial thickness, h/d , of 1.7. This suggests that a combination of frictional jamming and close packing considerations prevents efficient shear thinning of layers with $m = 1.25$ and 1.5. For layers with $m \geq 2$, the situation is quite different. Here, $\phi \geq 0.46$, which is higher than even the densest layers with $m < 2$. We posit that h_{ss} for layers with $1 < m < 2$, is determined by a small fraction of grains that are unable to drop into an open site on the layer, thus resulting in a relatively low packing fraction. These layers are jammed in the sense that the grains are trapped by neighboring grains, which cannot move due to lack of a spatially-coherent rolling moment and/or in-plane grain networks that distribute force, and these trapped grains apparently extend across the whole layer for $m \geq 2$.

We can also consider the possibility of force networks and the spatial variability of stress in our layers, topics which are of considerable interest in bulk granular matter [9,11,17]. The nature of such force chains in thin layers subjected to shear along the layer plane has received less attention, and even their existence is not definite. Buckling and packing phase transitions in monolayers are expected to be spatially heterogeneous [20], which would cause force concentration and, hence a mechanism for generation of force networks. Although we do not observe interparticle forces directly, the low packing fractions of our layers with $m < 2$ suggests that forces are indeed spatially heterogeneous. Thus, the minimum effective length of an antiplane force chain in these special circumstances may be $< 2d$, which is quite short compared to results from bulk granular materials [17,23]. Furthermore, the fact that monolayers do not spontaneously compact under normal loads ≥ 750 kPa suggests that in-plane force networks may play a significant role in shear of thin layers.

In conclusion, our exploration of jamming in thin granular layers has demonstrated a clear transition between the rolling and jammed states, and shown that this transition has characteristic properties which distinguish it from the fully three-dimensional analogs. Further studies could include imaging of individual particles and their contact forces, which would elucidate the microscopic dynamics as well as the nature of the heterogeneous force networks in such systems.

This work was supported by NSF grants ANT-0538195 and EAR-0337627.

*cjm@geosc.psu.edu

- [1] B. Miller, C. O'Hern, and R. P. Behringer, *Phys. Rev. Lett.* **77**, 3110 (1996).
- [2] W. Losert, J.-C. Géminard, S. Nasuno, and J.P. Gollub, *Phys. Rev. E* **61**, 4060 (2000).
- [3] E. Aharonov and D. Sparks, *Phys. Rev. E* **60**, 6890 (1999).
- [4] I. Albert, P. Tegzes, B. Kahng, R. Albert, J. G. Sample, M. Pfeifer, A.-L. Barabasi, T. Vicsek, and P. Schiffer, *Phys. Rev. Lett.* **84**, 5122 (2000).
- [5] F. Dalton, F. Farrelly, A. Petri, L. Pietronero, L. Pitolli, and G. Pontuale, *Phys. Rev. Lett.* **95**, 138001 (2005).
- [6] S. Siavoshi, A. V. Orpe, and A. Kudrolli, *Phys. Rev. E* **73**, 010301 (2006); A. Orpe and A. Kudrolli, *Phys. Rev. Lett.* **98**, 238001 (2007).
- [7] C. Josserand, P.-Y. Lagrée, and D. Lhuillier, *Europhys. Lett.* **73**, 363 (2006).
- [8] A. Baldassarri, F. Dalton, A. Petri, S. Zapperi, G. Pontuale, and L. Pietronero, *Phys. Rev. Lett.* **96**, 118002 (2006).
- [9] K. Mair and J. F. Hazzard, *Earth Planet. Sci. Lett.* **259**, 469 (2007).
- [10] D. S. Grebenkov, M. P. Ciamarra, M. Nicodemi, and A. Coniglio, *Phys. Rev. Lett.* **100**, 078001 (2008).
- [11] M. G. Clerc, P. Cordero, J. Dunstan, K. Huff, N. Mujica, D. Risso, and G. Caras, *Nature Phys.* **4**, 249 (2008).
- [12] M. Schmidt and H. Löwen, *Phys. Rev. Lett.* **76**, 4552 (1996).
- [13] L. E. Silbert, D. Ertas, G. S. Grest, T. C. Halsey, and D. Levine, *Phys. Rev. E* **65**, 031304 (2002).
- [14] C. O'Hern, L. E. Silbert, A. J. Liu, and S. R. Nagel, *Phys. Rev. E* **68**, 011306 (2003).
- [15] E. I. Corwin, H. M. Jaeger, and S. R. Nagel, *Nature (London)* **435**, 1075 (2005).
- [16] O. Dauchot, G. Marty, and G. Biroli, *Phys. Rev. Lett.* **95**, 265701 (2005).
- [17] T. S. Majmudar, M. Sperl, S. Luding, and R. P. Behringer, *Phys. Rev. Lett.* **98**, 058001 (2007).
- [18] H. P. Zhang and H. A. Makse, *Phys. Rev. E* **72**, 011301 (2005).
- [19] S. Henkes and B. Chakraborty, *Phys. Rev. Lett.* **95**, 198002 (2005).
- [20] S. Naser, C. Bechinger, P. Leiderer, and T. Palberg, *Phys. Rev. Lett.* **79**, 2348 (1997).
- [21] J. L. Anthony and C. Marone, *J. Geophys. Res.* **110**, B08409 (2005).
- [22] F. da Cruz, S. Emam, M. Prochnow, J.-N. Roux and F. Chevoir, *Phys. Rev. E* **72**, 021309 (2005).
- [23] M. Muthuswamy and A. Tordesillas, *J. Stat. Mech.* (2006) P09003.